

## **General Disclaimer**

### **One or more of the Following Statements may affect this Document**

- This document has been reproduced from the best copy furnished by the organizational source. It is being released in the interest of making available as much information as possible.
- This document may contain data, which exceeds the sheet parameters. It was furnished in this condition by the organizational source and is the best copy available.
- This document may contain tone-on-tone or color graphs, charts and/or pictures, which have been reproduced in black and white.
- This document is paginated as submitted by the original source.
- Portions of this document are not fully legible due to the historical nature of some of the material. However, it is the best reproduction available from the original submission.

X-621-71-141  
PREPRINT

NASA TM X- 65500

# MAGNETIC STORM EFFECTS IN THE NEUTRAL COMPOSITION

H. G. MAYR  
H. VOLLAND

FACILITY FORM 602

N71 23366

(ACCESSION NUMBER)

(THRU)

G3

(PAGES)

TMX 65500

(CODE)

13

(NASA CR OR TMX OR AD NUMBER)

(CATEGORY)

FEBRUARY 1971



— GODDARD SPACE FLIGHT CENTER —  
GREENBELT, MARYLAND

X-621-71-141  
Preprint

MAGNETIC STORM EFFECTS ON THE NEUTRAL COMPOSITION

by

H. G. Mayr and H. Volland\*

Thermosphere and Exosphere Branch

February 1971

---

\*University of Bonn, West Germany.

### ABSTRACT

The thermospheric wind circulation, excited during magnetic storms presumably by joule heating within the auroral zone, is shown to be an effective mechanism for removing atomic oxygen at high latitudes. Wind induced variations in O exceed the temperature effects up to 250 km. The calculated depletion is most pronounced at around 180 km where the density can decrease by as much as a factor of two, consistent with the observed storm time variations in the ionosphere. At higher altitudes, this effect is canceled by the thermal expansion in atomic oxygen thus explaining the negligible response in the concentration of this atmospheric constituent under distributed conditions when  $N_2$  increased by as much as a factor of ten.

## MAGNETIC STORM EFFECTS IN THE NEUTRAL COMPOSITION

by

H. G. Mayr and H. Volland

### I. INTRODUCTION

Reber et al. 1970 and Taeusch and Carignan 1970, have presented mass spectrometer measurements of  $N_2$  and O from OGO 6 during magnetic storms. These data show at heights of typically 400 km the following characteristics:

1. A gradual increase in the  $N_2$  concentration from low to high latitudes (up to a factor of 10 for  $A_p \sim 200$ ),
2. An increase in the exospheric temperature (from  $1000^\circ$  up to  $1400^\circ$ ) at high altitudes which was inferred from the variations in  $N_2$ .
3. Negligible variations in O with some tendency to decrease at high latitudes where  $N_2$  showed significant enhancements.

The obvious implication is that during magnetic storms a considerable amount of energy is deposited in the auroral zone presumably below 200 km thus causing a thermal expansion in  $N_2$  which is the major constituent in the lower thermosphere.

Associated with this temperature enhancement, O should increase similarly if, as present models assume, the composition did not vary at the turbopause level. This is contrary to the observed behavior in atomic oxygen which, if anything, tends to decrease in the region of enhanced temperatures.

Thus we suggest that the magnetic storm heating produces changes in the neutral composition and in particular a decrease of the relative concentration of O within the lower thermosphere. In this paper, we shall discuss a model that can explain such variations in terms of diffusion processes associated with the thermospheric circulation that is excited in an altitude range where joule dissipation (Cole, 1970) is most likely the predominant heat source.

## II. THEORY

The thermospheric winds up to 250 km, where  $N_2$  is the major constituent, exert drag forces on the minor species O in this region. The diffusion velocities induced by this interaction upset the static equilibrium for atomic oxygen thus producing variations in the relative concentration of O to  $N_2$ . This process has been studied for seasonal variations in the annual component (Kellogg, 1961) and semiannual component (Mayr and Volland, 1970).

Magnetic storms have time scales of typically one day which are quite different from the periods of half a year in the seasonal variations, and this reflects significantly upon the atmospheric properties. One can estimate (e.g. at 120 km) the characteristic times for diffusion of O through  $N_2$

$$\tau_D \sim \frac{H^2}{D} \sim 6 \text{ days}$$

and for the mass transport due to horizontal winds

$$\tau_u \sim \frac{R}{V} \sim 5 \text{ days}$$

where  $H$  (10 km) is the density scale height,  $D$  ( $6 \times 10^6$ ) the diffusion coefficient,  $V$  (10 m/sec) the wind velocity and  $R$  the earth's radius.

Seasonal variations in the wind field and in the diffusion transport can easily be excited even at the turbopause level. The response of the neutral atmosphere is almost instantaneous on this time scale thus the continuity equations can be treated as time independent. As a consequence, a unique relation evolves between the vertical and horizontal wind velocities with upward winds reducing atomic oxygen and downward winds enhancing it (Mayr and Volland, 1970).

In contrast, magnetic storm variations with a time scale of about one day, comparable to the response time of the atmosphere, cannot be excited readily at all altitudes. The response time of the wind field and the phase difference between vertical and horizontal winds increase significantly at low altitudes. The relatively long diffusion time causes further delay in the response of the composition to the vertical and horizontal wind fields; so it is obvious that the transient aspects of the magnetic storm variations must be important.

We shall therefore address ourselves to the following questions: can the wind fields during magnetic storms produce variations in the composition that are consistent with the observations and b) what inferences can be made on the energy source from the time response of the composition?

#### The Model of Volland and Mayr (1971)

The bulk motion of  $N_2$  up to 250 km where this species dominates constitute the wind field that affects the O concentration. As a major constituent,  $N_2$  is not significantly influenced by diffusion. Furthermore, the energy sources that

determine essentially these dynamics are within the  $N_2$  region up to 250 km. For these reasons, the wind field can be computed without considering diffusion processes. However, the wind fields at higher altitudes where O is the major constituent is of course affected by these processes. This aspect will be discussed with some of its consequences in a subsequent paper.

Volland and Mayr (1971 a,b) have treated the dynamic of the neutral atmosphere in response to auroral heating. Although the calculations cover an altitude range up to 400 km diffusion has not been considered. For reasons outlined before, however, their results are completely valid within the  $N_2$  region of the thermosphere and thus can be adopted to study the diffusion properties of O. A brief summary of this model is therefore here appropriate.

Assuming an energy source that is confined to the auroral zone, Volland and Mayr expanded this input into a series of spherical harmonics

$$Q = Q_0 (P_0 + 3.66 P_2 + 2.22 P_4 - 2.65 P_6 - 6.91 P_8 \dots) \quad (1)$$

As expected, this series converges slowly. The model shows however, that the response of the neutral atmosphere to the various energy components is such that the higher wave numbers are rapidly damped. This is illustrated in Fig. 1 (corresponding to Fig. 2 in their paper) which shows the transfer function  $G_n$  that relates density ( $\rho_n$ ) and energy ( $Q_n$ ) variations over a wide frequency range through

$$\rho_n \equiv G_n Q_n, \quad (2)$$

thus describing the efficiency for the excitation of the various components. As is evident from this figure, the efficiency decreases with the power of  $1/n^2$  for

frequencies that correspond to magnetic storm periods of typically one day ( $\omega = 7.3 \times 10^{-5}$  /sec). This clearly implies that only the first two harmonics  $P_0$  and  $P_2$  in the energy expansion are most effective in exciting density variations, a fact that is supported by measurements that show a strong worldwide component ( $P_0$ ) in the magnetic storm response of the thermosphere and a gradual increase toward higher latitudes ( $P_2$ ) in the  $N_2$  concentration (Taeusch and Carignan, 1971). Thus we shall confine ourselves in this paper to treat only the  $P_0$  and  $P_2$  components of the energy input as they excite winds and consequently variations in the composition.

### The Diffusion Model

The continuity equations for mass and momentum conservation are

$$\begin{aligned}
 2q [O_2] - [O] [N_2] (2\alpha_1 [O] + \alpha_2 [O_2]) - \\
 - \frac{\partial}{\partial r} ([O] v_{or}) - \frac{1}{r \sin \theta} \frac{\partial}{\partial \theta} ([O] \sin \theta v_{\theta\theta}) - \\
 - \frac{1}{r \sin \theta} \frac{\partial}{\partial \lambda} ([O] v_{\theta\lambda}) = \frac{\partial}{\partial t} [O]
 \end{aligned} \tag{2}$$

$$\begin{aligned}
 [O] (v_{or} - v_r) - D \left( \frac{\partial [O]}{\partial r} + \frac{[O]}{T} \frac{\partial T}{\partial r} + \frac{mg}{kT} [O] \right) \\
 - K \left( \frac{\partial [O]}{\partial r} + \frac{[O]}{T} \frac{\partial T}{\partial r} + \frac{\bar{m}g}{kT} [O] \right)
 \end{aligned} \tag{3}$$

$$(v_{\theta\theta} - v_\theta) = 0 \tag{4}$$

$$(v_{\theta\lambda} - v_\lambda) = 0 \tag{5}$$

where

$k$  = Boltzmann constant

$q$  = photo production rate due to dissociation of  $O$

$\alpha_1$  = rate of three body recombination ( $O + O + N_2 \rightarrow O_2 + N_2$ )

$\alpha_2$  = rate of three body recombination ( $O + O_2 + N_2 \rightarrow O_3 + N_2$ )

$[O]$ ,  $[O_2]$ ,  $[N_2]$  = number densities for  $O$ ,  $O_2$  and  $N_2$

$V_{0r}$ ,  $V_{0\theta}$ ,  $V_{0\lambda}$  = transport velocities for  $O$  in the radial ( $r$ ), colatitudinal ( $\theta$ ) and longitudinal ( $\lambda$ ) direction.

$V_r$ ,  $V_\theta$ ,  $V_\lambda$  = wind components for the three directions

$D$  = molecular diffusion coefficient for  $O$  through  $O_2$  and  $N_2$

$K$  = Eddy diffusion coefficient

$t$  = universal time.

$m, \bar{m}$  = mass of atomic oxygen, mean molecular mass

$g$  = gravitational acceleration

In the latitudinal and longitudinal directions the drag terms  $[O] (V_{0\theta} - v_\theta)$  and  $[O] (V_{0\lambda} - v_\lambda)$  dominate the lateral momentum transfer thus reducing to the simplified equations (4) and (5). The inertia terms  $\partial/\partial t (V_{0r}, V_{0\theta}, V_{0\lambda})$  have been neglected in Equations 3 through 5 since they are negligible when compared with accelerations due to the pressure gradients.

In order to solve these equations, a number of simplifying assumptions were made:

1. The local time and longitude dependences are neglected
2. The variables are separated into storm time  $t$ , colatitude  $\theta$ , and altitude

$r$  components in the form

$$[O] = [O]_0(r) + [O]_2(r) P_2(\theta) e^{j\omega(t-\phi_0)} \quad (6)$$

for atomic oxygen, and

$$\begin{aligned}
 F &= [O] (V_{0r} - V_r) \\
 &= F_0(r) + F_2(r) P_2(\theta) e^{j\omega(t-\phi_F)}
 \end{aligned} \tag{7}$$

for the diffusion flux. The subscripts 2 refer to the second spherical harmonic

$$P_2(\theta) = \frac{1}{2} (3 \cos^2 \theta - 1).$$

We choose the predominant Fourier component for the magnetic storm variations thus adopt a frequency  $\omega$  with a period of typically one day.

3. From the model of Volland and Mayr (1971, b), which applies full wave calculations to the atmospheric dynamics, the appropriate forms for the wind and temperature fields are adopted.

$$V_r = V_{r2}(r) P_2(\theta) e^{j(\omega t - \phi_r)} \tag{10}$$

$$V_\theta = V_{\theta 1}(r) \sin \theta P_1(\theta) e^{j(\omega t - \phi_\theta)} \tag{11}$$

with

$$P_1(\theta) = \cos(\theta),$$

and

$$T = T_0(r) + T_2(r) P_2 e^{j\omega(t-\phi_T)} \tag{12}$$

4. Assuming that higher order terms in the frequency and latitude expansions can be neglected, perturbation theory is applied which leads in a straight forward manner to a set of first order differential equations

$$\frac{\partial}{\partial r} (F_0) + \alpha_1 [O]_0^2 [N_2] + \alpha_2 [O]_0 [O_2] [N_2] - 2\alpha [O_2] = 0 \tag{13}$$

$$F_0 + (D + K) \left( \frac{\partial [O]_0}{\partial r} + \frac{[O]_0}{T_0} \frac{\partial T_0}{\partial r} + \frac{[O]_0}{kT_0} \frac{g(mD + mk)}{D + k} \right) = 0 \quad (14)$$

$$\begin{aligned} \frac{\partial f}{\partial r} + \frac{1}{[O]_0} \frac{\partial [O]_0}{\partial r} f + (2a_1 [O]_0 + a_2) \rho - j\omega \rho \\ = - \frac{1}{[O]_0} \frac{\partial}{\partial r} ([O]_0 v_{r2}) - \frac{2}{r} v_{\theta 1} \end{aligned} \quad (15)$$

$$\begin{aligned} \frac{\partial \rho}{\partial r} + \frac{1}{(D + K)} f + \left( \frac{1}{[O]_0} \frac{\partial [O]_0}{\partial r} + \frac{1}{T_0} \frac{\partial T_0}{\partial r} + \frac{g}{kT_0} \frac{(mD + mK)}{D + K} \right) \rho = \\ = - \left( \frac{1}{T_0} \frac{\partial T}{\partial r} - \frac{1}{T_0^2} \frac{\partial T_0}{\partial r} T - \frac{g}{kT_0^2} \left( \frac{mD + mK}{D + K} \right) T \right) \end{aligned} \quad (16)$$

with

$$e = \frac{f_2}{F_0} e^{j\omega(t - \varphi_F)} \quad (17)$$

$$\rho = \frac{[O]_2}{[O]_0} e^{j\omega(t - \varphi_0)} \quad (18)$$

$$\frac{1}{H} = \frac{1}{N} \frac{\partial N}{\partial r} \quad (19)$$

where N is the atmospheric density.

The equations (13) and (14) describe the steady state distribution for atomic oxygen without being affected by winds and temperature variations. As these equations do not depend on the other variables, they can be solved independently. Such a solution has been described e.g. in Mayr and Volland (1970) and it is here adopted as input.

The equations (15) and (16), which are complex and represent therefore four equations, are then solved by means of a trial and error scheme with the following boundary conditions:

a. At heights above 250 km, O becomes the major constituent, therefore diffusion is negligible

$$f = 0 \quad \text{at} \quad 250 \text{ km}$$

b. The diffusion time increases at altitudes below 100 km to four days, thus the temporal variations must be small there. To account for that, it is assumed arbitrarily that

$$p = 0 \quad \text{at} \quad 90 \text{ km.}$$

This implies that the solution is meaningless at this altitude level. However, at heights above 100 km, the solution is very insensitive to this artificial constraint thus the solution can be considered as unique there.

The equations (15) and (16) have the important characteristic that the complex variables  $f$  and  $p$  depend linearly on the temperature  $T_2$  and wind fields  $V_{r2}$  and  $V_{\theta 1}$ . This implies that the effects induced by temperature and wind variations can be separated thus providing a means of identifying their relative significance.

Considering furthermore that the temperature and wind fields from the model of Volland and Mayr (1971 b) also depend linearly on the energy input, a linear relationship between variations in the composition and heat source evolves which greatly simplifies the discussion.

### III. DISCUSSION

Two significantly different heating mechanisms have been proposed for geomagnetic storms in the Auroral zone:

a. Heating due to particle precipitation, a process in which recombination, electron heating and vibrational excitation of  $N_2$  produce a heat input that peaks at about 100 km or above, depending upon the energy of the precipitating electrons. (Rees, private communication.)

b. Joule heating due to electric fields that are generated in the magnetosphere (Cole, 1970). Particle precipitation contributes to this heat source by enhancing the conductivity through impact ionization. This energy input peaks in the E region presumably at about 150 km (Cole, 1970).

It seems obvious that both mechanisms should be active. The difference in the height distribution for both heat inputs, however, suggests significantly different responses in the thermosphere dynamics. Thus the question arises whether the observed effects in the composition can be tied (through our models) to one particular heat source?

Two energy models, shown in Fig. 2 are adopted. The form of the distributions is the same, however the energy peaks are placed at 100 and 150 km. As we deal here with a linear theory, the absolute magnitudes of the heat input is

insignificant at this point. The relative magnitudes of the  $P_0$  and  $P_2$  components are chosen in accordance with the spherical expansion (1)

$$Q_2 = 3.66 Q_0.$$

With these inputs, the temperature and wind fields are computed from the three dimensional model of Volland and Mayr (1971, b) for the predominant frequency of a typical magnetic storm ( $\omega = 2\pi/1$  day). As we restrict ourselves here to the dominating frequency we make a very rough approximation to the impulse type heat input in the Auroral zone. For this reason our present analysis cannot account for details in the time evolution of the storm time dynamics.

The results show that the uniform (one dimensional) expansion for the  $Q_0$  component produces vertical (only) wind velocities that are one order of magnitude smaller than the vertical wind velocities for the non-uniform and two dimensional  $P_2$  component, while the temperature amplitude is somewhat larger for the  $Q_0$  term. As we are primarily interested in wind-diffusion effects competing with the temperature induced variations in the composition, we conclude that the  $Q_0$  component-equivalent to a one-dimensional approximation - does not contribute appreciably to the dynamics and diffusion in the thermosphere. Therefore, we can disregard the  $Q_0$  term.

#### Wind Effects

Fig. 3 shows the magnitudes of the vertical and meridional wind velocities and temperature fields computed from the model of Volland and Mayr (1971, b) for the  $Q_2$  component. Figs 3a and 3b represent the solutions for energy inputs that peak at 100 km and 150 km respectively (see Fig. 2).

The wind direction is upward (positive) for the vertical wind field in Figs. 3a and 3b at the time of the maximum Auroral heat input. At the same time the meridional wind direction is equatorward (positive) at heights of the energy maximum and above (that is above 100 km for Fig. 3a and above 130 km for Fig. 3b). Below 130 km the winds blow toward the poles for case b.

With these inputs, the diffusion equations (15) and (16) are solved. Fig. 4a describes amplitudes and phase of the variations in atomic oxygen for the vertical and meridional wind components and for the combination of both. These variations are excited by a heat input that peaks at 100 km. Fig. 4b describes these parameters for the energy maximum at 150 km. The time of the density maxima is plotted with respect to the time of the maximum auroral heat input.

The most interesting feature in the comparison between both solutions – that show the combined wind effect (solid lines in Fig. 4) for these energy models – is the phase relation. In both cases, the phase is very similar below 120 km. Above 140 km, however, a phase difference of nearly 12 hours develops thus indicating that the effects go in opposite directions. As is evident, the maximum in atomic oxygen occurs essentially at the time of the maximum auroral heat input (Fig. 4a) in the case where the wind field is excited at 100 km. For the 150 km heat input, this maximum occurs 12 hours ( $180^\circ$ ) earlier and this implies that a minimum develops in atomic oxygen during the time of magnetic storms.

The reasons for this difference in the response of the neutral composition are somewhat complex. The vertical and meridional wind velocities enter the diffusion equation (15) in the form

$$V_{r2} \left( \frac{1}{H_0} - \frac{1}{H_v} \right) - \frac{2}{r} V_{\theta 1} = S \quad \begin{array}{l} > 0 \text{ (source)} \\ < 0 \text{ (sink)} \end{array} \quad (20)$$

where

$$H_0 = [O]_0 / \frac{\partial [O]_0}{\partial r} \text{ (oxygen scale height)}$$

and

$$H_v = V_{r2} / \frac{\partial V_{r2}}{\partial r} \text{ (scale height of the vertical winds)}$$

In Fig. 3 the meridional velocity  $V_{\theta 1}$  is positive (except below 130 km in Fig. 3b and there the wind velocity decreases rapidly). For this reason, this wind component acts as a sink which removes atomic oxygen at high altitudes. This is reflected both in Figs. 4a and 4b where the component  $(\Delta O)_{V_{\theta 1}}$  is shifted to earlier hours thus producing a minimum in atomic oxygen at or after the time of the maximum energy input. At heights below 140 km, the phase is shifted progressively to later hours at lower heights thus reflecting the increasing response time in the lower thermosphere.

The effects of the vertical wind velocity depend on its scale height,  $H_v$  (see Eq. 20). When the vertical wind velocity increases more rapidly than atomic oxygen is decreasing with height the wind effectively removes oxygen; otherwise it supplies atomic oxygen. In this respect, particularly the wind fields - excited at 100 and 150 km - are very different.

In the regions around the energy source and up to about 130 km atomic oxygen is removed to be supplied over the entire altitude range between 130 and 250 km (for Fig. 4a). Above 130 km the vertical wind constitutes a source that accumulates

oxygen during storm times. This is reflected in both, the relatively large amplitude of  $(\Delta O)_{V_{r2}}$  (which surpasses the component  $(\Delta O)_{V_{\theta1}}$ ) and in the occurrence of the density maximum after the time of the maximum energy input. Both wind components  $(\Delta O)_{V_{\theta1}}$  and  $(\Delta O)_{V_{r2}}$  are out of phase by almost  $180^\circ$  thus opposing each other. The predominance of the  $(\Delta O)_{V_{r2}}$  term therefore produces a slight enhancement in atomic oxygen during storm time (see the phase and amplitude of  $(\Delta O)_{wind}$  in Fig. 4a). This is opposite to the variations in the composition that are inferred from storm time measurements. Below 130 km the steep gradient in  $V_{r2}$  causes a depletion of atomic oxygen which is reflected in the decrease of the amplitude  $(\Delta O)_{V_{r2}}$  and in the shift of its phase to earlier hours. The superposition of  $(\Delta O)_{V_{r2}}$  and  $(\Delta O)_{V_{\theta1}}$  produces then the structure in  $(\Delta O)_{wind}$  within the lower thermosphere.

In the case where the energy source peaks at 150 km, the vertical wind component removes atomic oxygen up to 170 km and supplies it over an altitude range of only 50 km above that height. The net effect is a relatively small accumulation of O above 150 km which is reflected in amplitude and phase of  $(\Delta O)_{V_{r2}}$  (illustrated in Fig. 4b). In contrast to Fig. 4a, the effect of the vertical wind field is here considerable smaller than that of the meridional wind velocity. Consequently, the depletion of O due to meridional winds dominates (see  $(\Delta O)_{wind}$  in Fig. 4b) and O decreases during storm time.

Below 170 km, the effects are similar to the ones below 130 km which were described in Fig. 4a.

Finally, a very important feature in the comparison between both models is related to the values of the phase. For the energy source at 100 km, the

vertical wind velocity produces a peak and the meridional wind a minimum in O five hours after the storm above 140 km. With the energy input at 150 km, the phase difference is only an hour, thus contributing to the depletion of O at the time of the magnetic storm. This difference simply reflects the decrease of the response time in the neutral atmosphere at higher altitudes.

#### Comparison Between Temperature and Wind Effects

In Figs. 5a and 5b, we show the variations in O due to the thermal expansion  $(\Delta O)_T$  (computed from Eq. 15 and 16), and compare them with the wind induced components that were discussed before. Furthermore, we plotted the variations in  $N_2$ . In order to cover the altitude range shown in these figures, we have assumed that the wind effects are negligible above 250 km. Therefore phase and amplitude  $(\Delta O)_{wind}$  remain constant.  $(\Delta O)_T$  was deduced above 250 km by considering the diffusion equations that express the state of hydrostatic equilibrium there. The distributions in  $N_2$  were adopted from the total atmospheric density up to 250 km in the three dimensional model of Volland and Mayr (1971, b) and they were extrapolated above 250 km under the assumption of diffusive equilibrium. Figs. 5a and 5b show the two models for energy maxima at 100 and 150 km.

It is apparent from these results that the magnitudes of the wind induced variations in atomic oxygen are comparable or even exceed the temperature components.

Above 200 km, the thermal expansion causes in both models a maximum in O at the time of the maximum auroral heat input. This is in phase with the time variation of  $N_2$ . Below 200 km, the phases of the temperature components shift in accordance with the phase and height gradients of the temperature field.

The superpositions of the temperature and wind components in the variations of atomic oxygen are shown as thick lines with the annotation  $\Delta O$ .

For the energy input at 100 km, the amplitude increases with height after showing a structure below 140 km which is somewhat similar to the variations in  $N_2$ .\*

The phase remains almost constant over the entire altitude range showing atomic oxygen to peak in phase with  $N_2$  at the time of the maximum heat input. Accordingly, we conclude that this energy model produces a composition effect that is contrary to the observations.

The results in Fig. 5b, for an energy maximum at 150 km are completely different. The amplitude peaks at 180 km with the phase at -12 hours. Thus atomic oxygen decreases and a minimum develops at the time of the storm. As is apparent in Fig. 5b, this effect is essentially induced by atmospheric winds. At higher altitudes, the temperature induced variations become more and more significant. Since temperature and wind effects go in opposite directions (see the phase difference of nearly 12 hours =  $180^\circ$ ) they cancel each other and thus produce the decrease in the amplitude and the gradual shift in the phase from -12 to -6 hours between 220 and 340 km. Above that height, the thermal expansion dominates the variations in O, thus causing some recovery in the amplitude and a further shift in the phase toward the phase of the temperature component at the time of the maximum energy input. As a result, the storm time increase at higher altitudes (~400 km) is significantly reduced which is in agreement with the observations by Reber, et. al. (1970) and Tausch and Carignan (1970).

---

\*This structure is of no significance; it reflects only the somewhat artificial boundary conditions in the wind model at 100 km which are damped out at higher altitudes.

Figure 6 summarizes these results. In altitude intervals of 100 km, we show the ratios

$$\left( \frac{[O]_0 + 2\Delta O P_2 e^{j\omega(t-\phi_0)}}{[O]_0} \right)$$

and

$$\left( \frac{[N_2]_0 + 2\Delta N_2 P_2 e^{j\omega(t-\phi_{N_2})}}{[N_2]_0} \right)$$

for  $t = 0$  (at the time of the maximum energy input), which reflect the relative variations in O and  $N_2$  during a magnetic storm.

It is apparent from this figure that  $N_2$  increases toward higher latitudes and at all altitudes thus showing the effect of the thermal expansion. In contrast, O is shown to decrease by about a factor of two at lower heights and at mid to high latitudes. This is consistent with the ionospheric analysis of Chandra and Herman (1969) who inferred a corresponding decrease of the O/ $N_2$  ratio during storms. At 300 km, no variation is apparent. At 400 km, O increases only slightly while  $N_2$  increases by about a factor of 10 from low to high latitudes; both features in O and  $N_2$  are in agreement with the observations of Tausch and Carignan, 1970.

To reproduce the observations, a peak energy input of

$$Q_2 = 0.49 \text{ erg/cm}^2 \text{ sec}$$

was required. Correspondingly, the global energy component is according to (1)

$$Q_0 = 0.13 \text{ erg/cm}^2 \text{ sec}$$

This energy input is comparable with the EUV heat source from the solar radiation.

#### IV. SUMMARY AND CONCLUSION

Fig. 7 summarizes in schematic form our model for the storm time variations in the neutral composition. The thermal expansion in  $N_2$ , most pronounced at high latitudes where the magnetic storm energies are dissipated, causes upwelling of air and meridional winds directed toward the equator. The diffusion velocities induced by these winds upset the static equilibrium for atomic oxygen and produce significant variations in its density distribution.

Our model studies have shown that with an energy source at 100 km associated with "hard" auroral precipitation (Rees, private communication), the upward transport of O predominates over the loss through meridional winds thus enhancing atomic oxygen at high latitudes during magnetic storms - which is in contrast to the observation

With the energy source at 150 km, presumably due to joule heating (Cole, 1970), the meridional wind component is more effective thus reducing atomic oxygen at high latitudes and transporting it to low latitudes. This process is most effective at altitudes around 200 km and it is consistent with the ionospheric observations suggesting a decrease of  $[O] / [N_2]$  during storms (Chandra and Herman, 1969).

At high altitudes, the thermal expansion in atomic oxygen becomes more important and this tends to cancel the wind effects. As a consequence, the storm time variations in O are negligible at altitudes above 300 km, which is consistent with the observations of Reber, et al. (1970) and Taeusch and Carignan (1970).

## V. REFERENCES

1. Chandra, S. and J. R. Herman, "F-Region Ionization and Heating During Magnetic Storms," Planet. Space Sci., 17, 841-851, 1960.
2. Cole, K. D., "Electrodynamic Heating and Movement of the Thermosphere," in press for Planet Space Sci., (1971).
3. Mayr, M. G. and H. Volland, "Semiannual Variations in the Neutral Composition," NASA Document X-621-70-478, Submitted for publication in Ann. Geophys.
4. Reber, C. A., A. E. Hedin, N. W. Spencer, D. N. Harpold, G. R. Carignan, and D. R. Tausch, "Neutral Atmospheric Composition Data from the Quadrupole Mass Spectrometer," EOS, 51, 1970.
5. Rees, M. M., Private Communication.
6. Tausch, D. R., and G. R. Carignan, "Neutral Composition Variations in the Auroral Zone During a Magnetic Storm," EOS, 51, 1970.
7. Volland, H., and H. G. Mayr, "The Response of the Thermospheric Density to Auroral Heating During Geomagnetic Disturbances," NASA Document X-621-71-57, accepted for publication in J. G. R. (1971).
8. Volland, H. and M. G. Mayr, "Three Dimensional Model of the Thermosphere, Part III Numerical Results," in preparation for publication (1971).

## VI. FIGURE CAPTIONS

1. The transfer functions,  $G_{ij}$ , from Volland and Mayr (1971, a) illustrating the efficiency for excitation of density components  $n_{ij}$  as a function of frequency.
2. Energy distributions used in computing the wind and temperature fields from the model of Volland and Mayr (1971, b).
- 3a. Amplitude of the vertical, ( $V_{r2}$ ), and meridional, ( $V_{\theta1}$ ), wind and temperature, ( $\Delta T$ ), fields computed from the model of Volland and Mayr for the energy maximum at 100 km.
- 3b. The same parameters as in 3a but for an energy source at 150 km.
- 4a. Relative amplitude and phase of the O variations induced by the vertical, ( $V_{r2}$ ), and meridional, ( $V_{\theta1}$ ), wind fields. The component with subscript, wind, shows the combined wind effect. The calculations were made for an energy input at 100 km.
- 4b. The same parameters as in 4a but for an energy source at 150 km.
- 5a. Amplitude and phase of the temperature, (T), and wind, (wind), components and the combination of both (without subscript). For comparison, the amplitudes and phase of the  $N_2$  concentration are shown. The results correspond to the heat input at 100 km.
- 5b. The same parameters as in Fig. 5a but for a heat source at 100 km.
6. The relative variations of O and  $N_2$  as functions of latitude at different heights. These results agree with observations of the composition and were

computed with an energy input that peaks at 150 km suggesting joule dissipation as the heating mechanism.

7. Schematic illustration of the model.

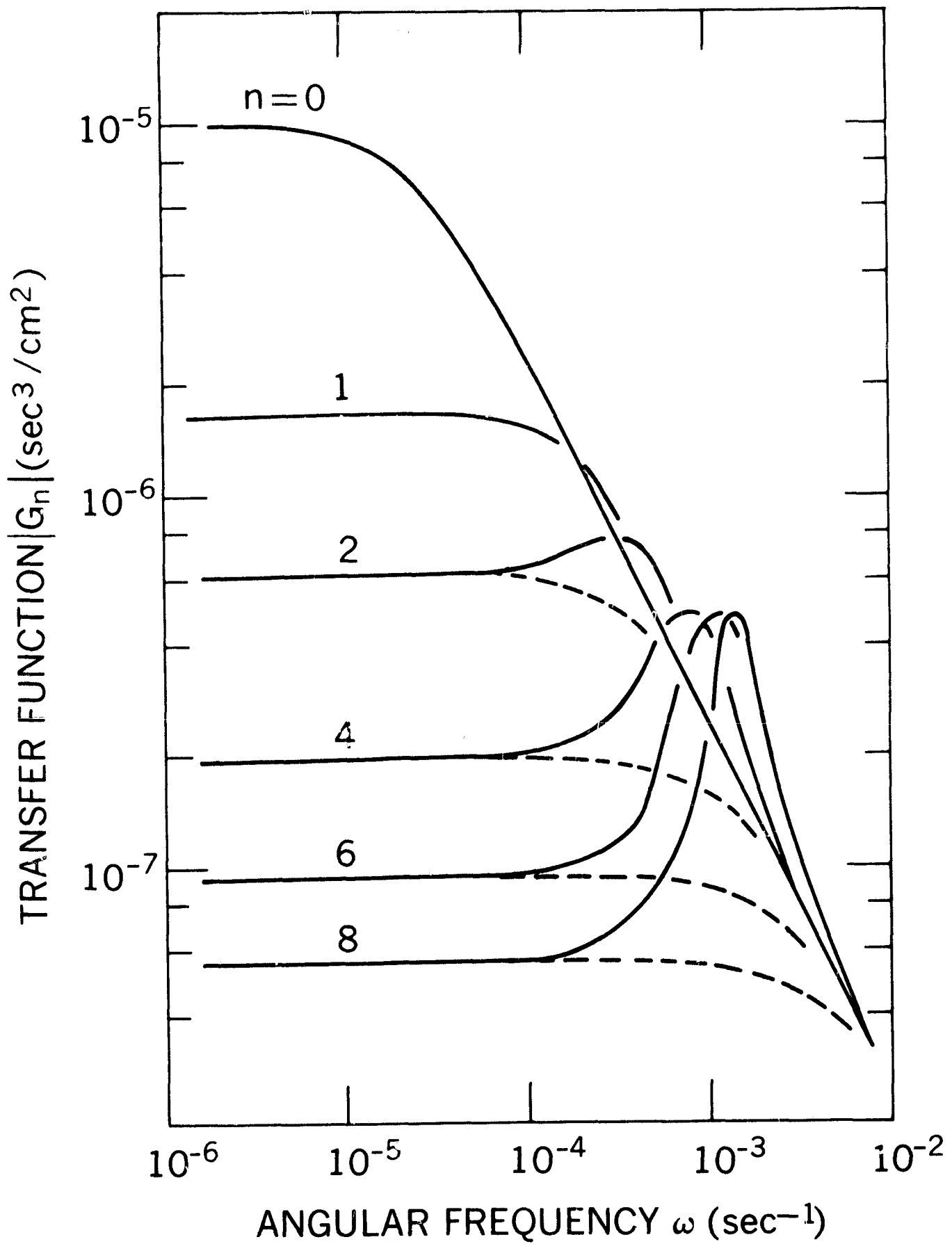


Figure 1. The transfer functions,  $G_n$ , from Volland and Mayr (1971, a) illustrating the efficiency for excitation of density components  $\rho_n$  as a function of frequency.

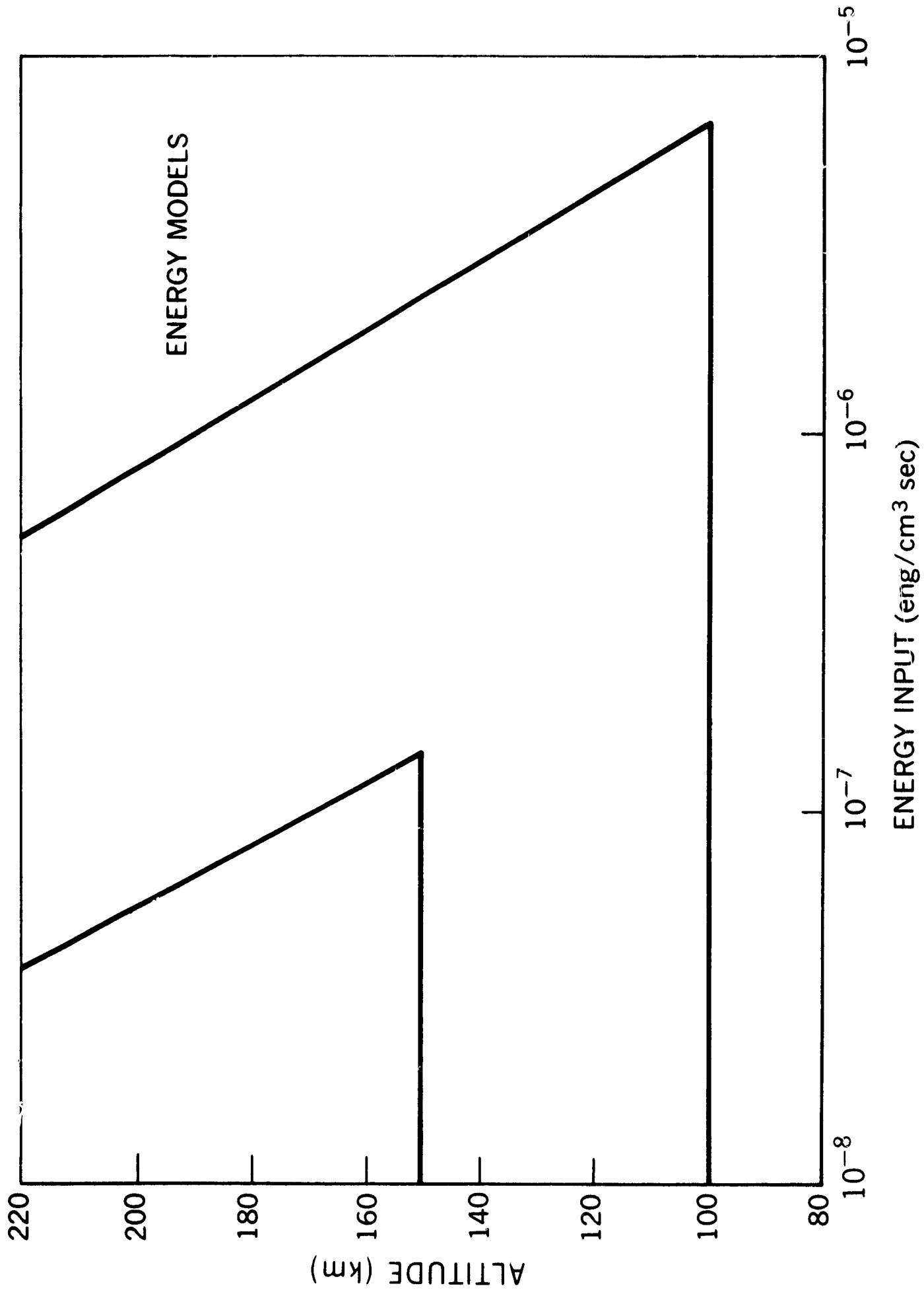


Figure 2. Energy distributions used in computing the wind and temperature fields from the model of Volland and Mayr.

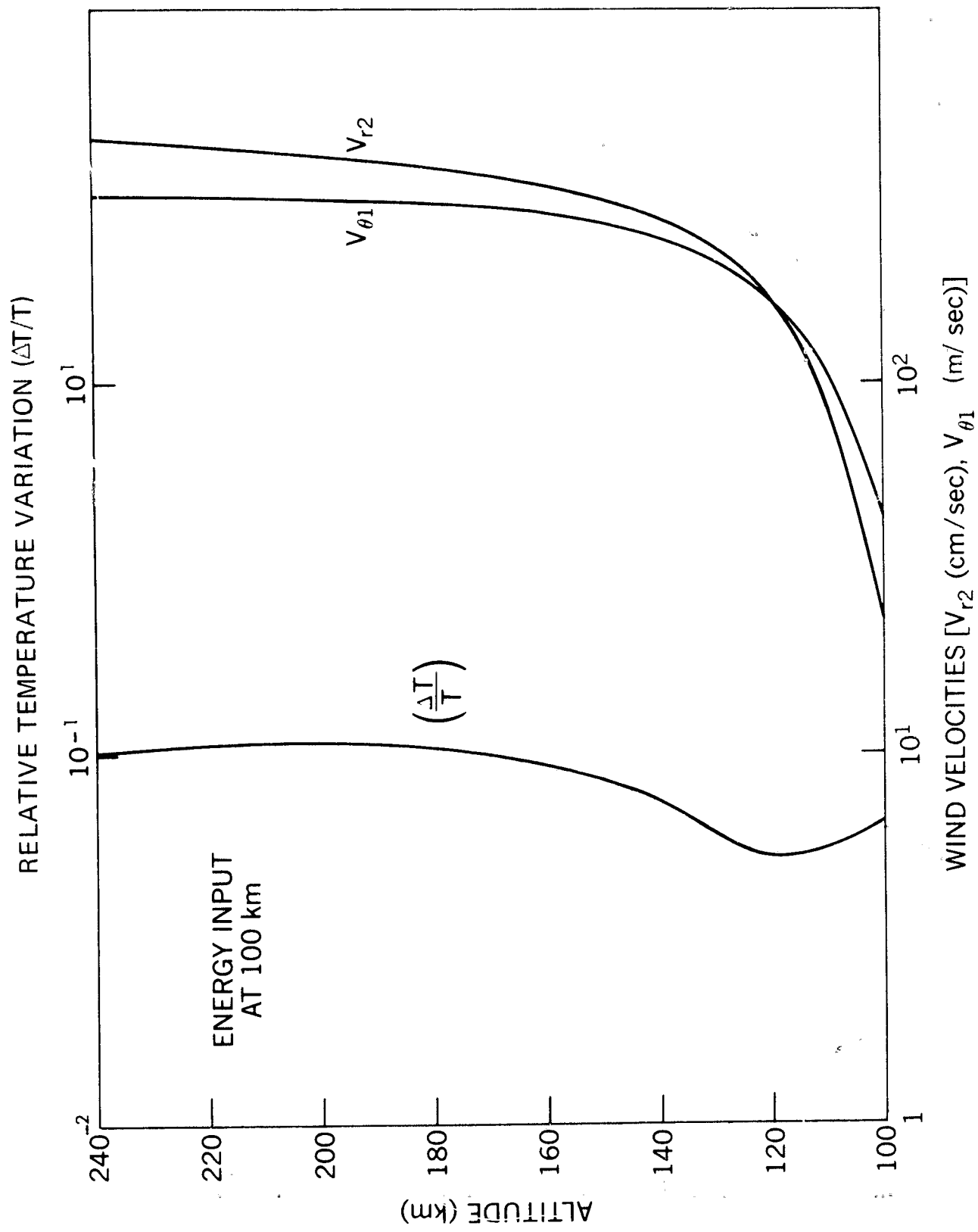


Figure 3a. Amplitude of the vertical, ( $V_{r2}$ ), and meridional, ( $V_{\theta 1}$ ), wind and temperature, ( $\frac{\Delta T}{T}$ ), fields computed from the model of Volland and Mayr for the energy maximum at 100 km.

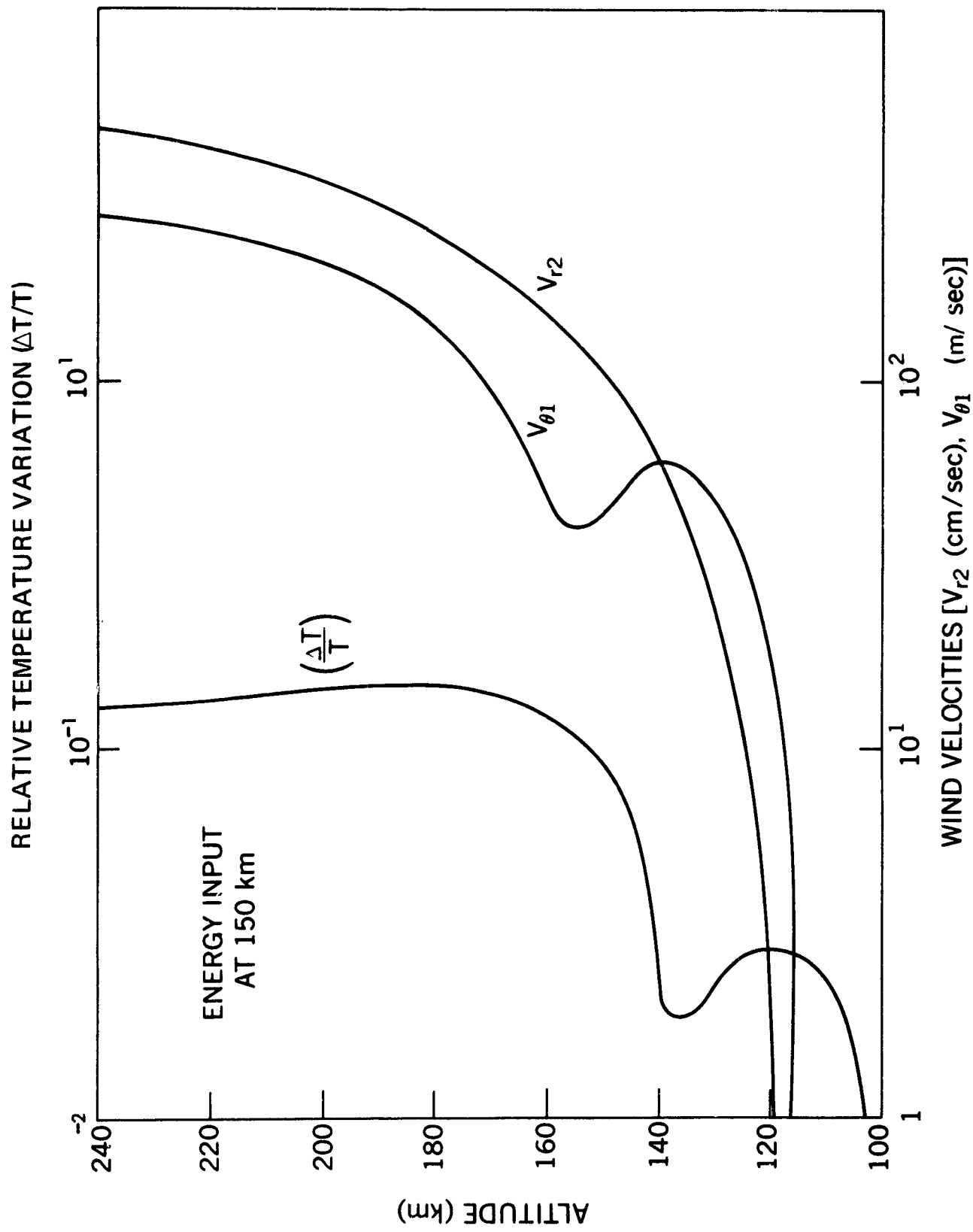


Figure 3b. Amplitude of the vertical, ( $V_{r2}$ ), and meridional, ( $V_{\theta 1}$ ), wind and temperature, ( $\Delta T$ ), fields computed from the model of Volland and Mary for the energy source at 150 km.

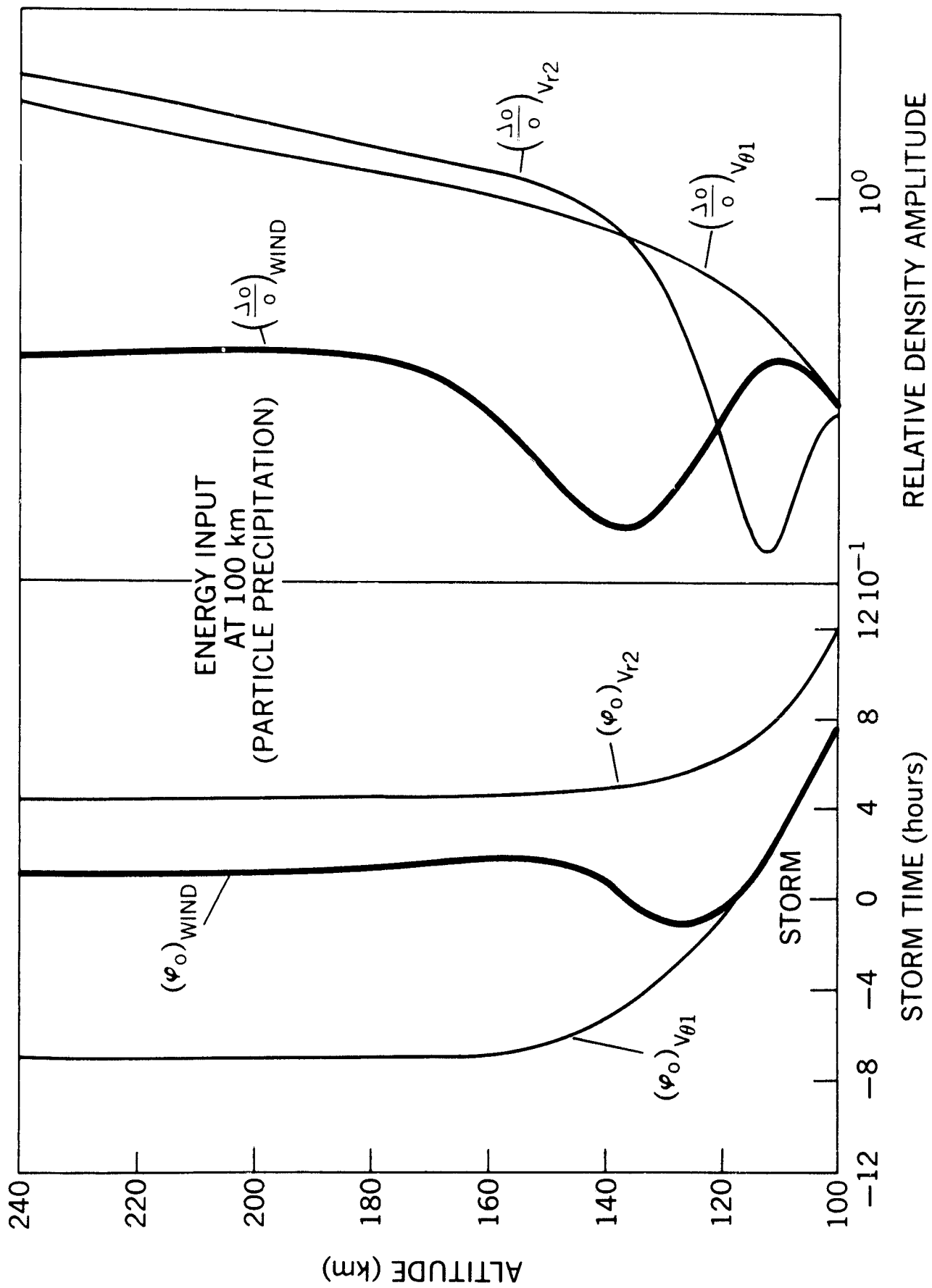


Figure 4a. Relative amplitude and phase of the O variations induced by the vertical, ( $V_{r2}$ ), and meridional, ( $V_{\theta1}$ ), wind fields. The component with subscript, wind, shows the combined wind effect. The calculations were made for an energy input at 100 km.

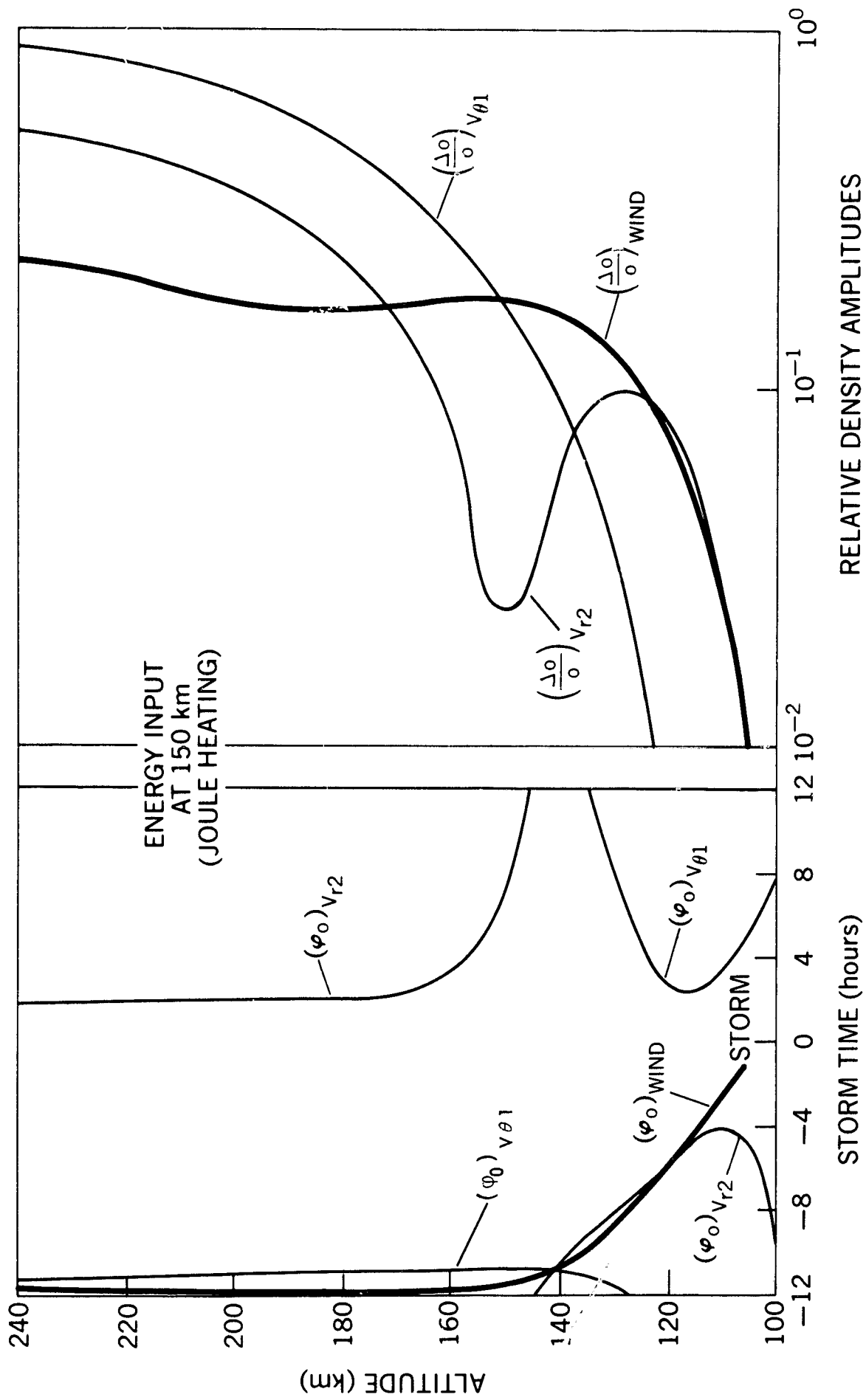


Figure 4b. Relative amplitude and phase of the O variations induced by the vertical, ( $V_{r2}$ ), and meridional, ( $V_{\theta 1}$ ), wind fields. The component with subscript, wind, shows the combined wind effect. The calculations were made for an energy source at 150 km.

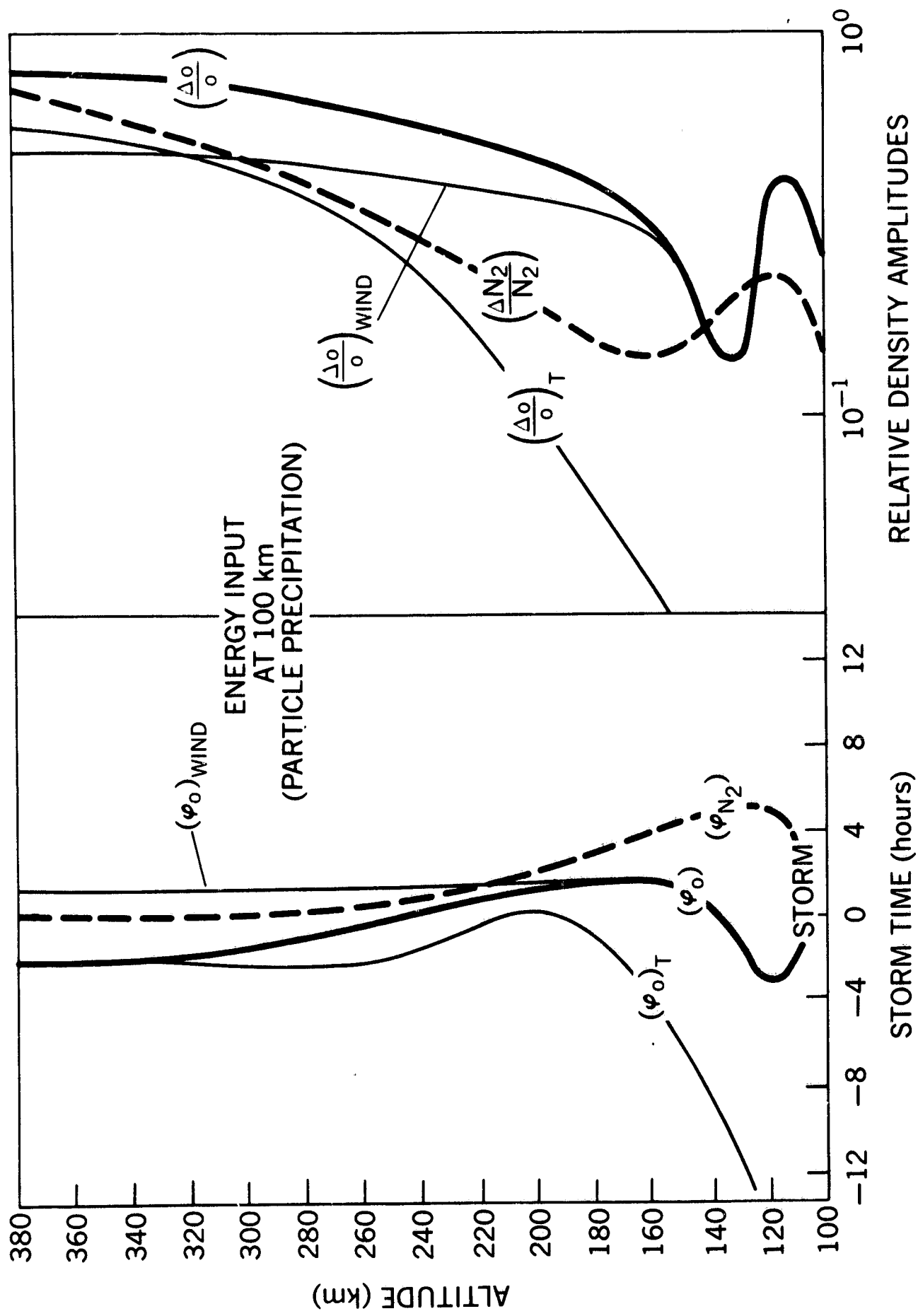


Figure 5a. Amplitude and phase of the temperature, (T), and wind, (wind), components and the combination of both (without subscript). For comparison, the amplitudes and phase of the  $N_2$  concentration are shown. The results correspond to the heat input at 100 km.

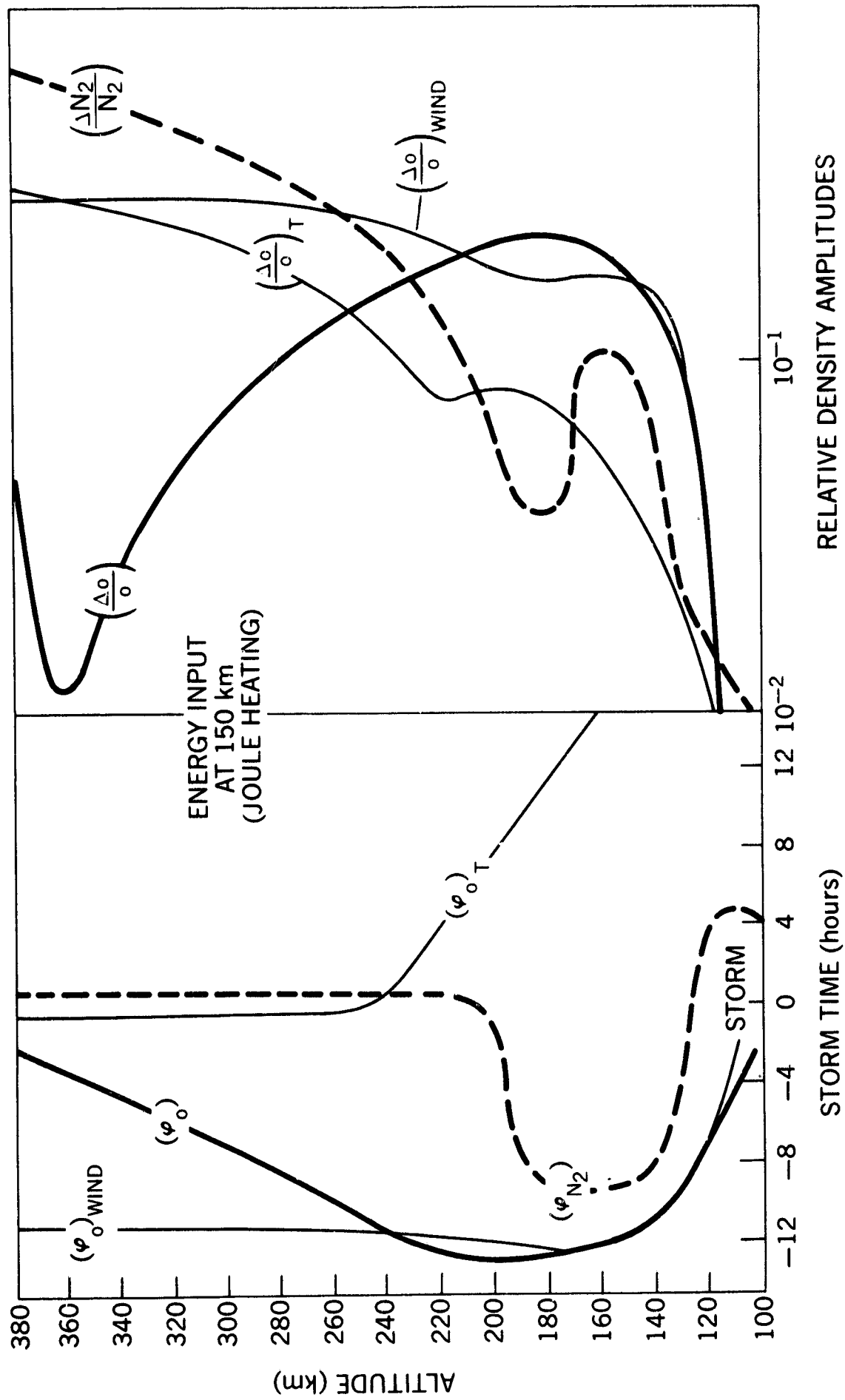


Figure 5b. Amplitude and phase of the temperature,  $(T)_r$  and wind,  $(\text{wind})_r$  components and the combination of both (without subscript). For comparison, the amplitudes and phase of the  $N_2$  concentration are shown. The results correspond to the heat source at 150 km.

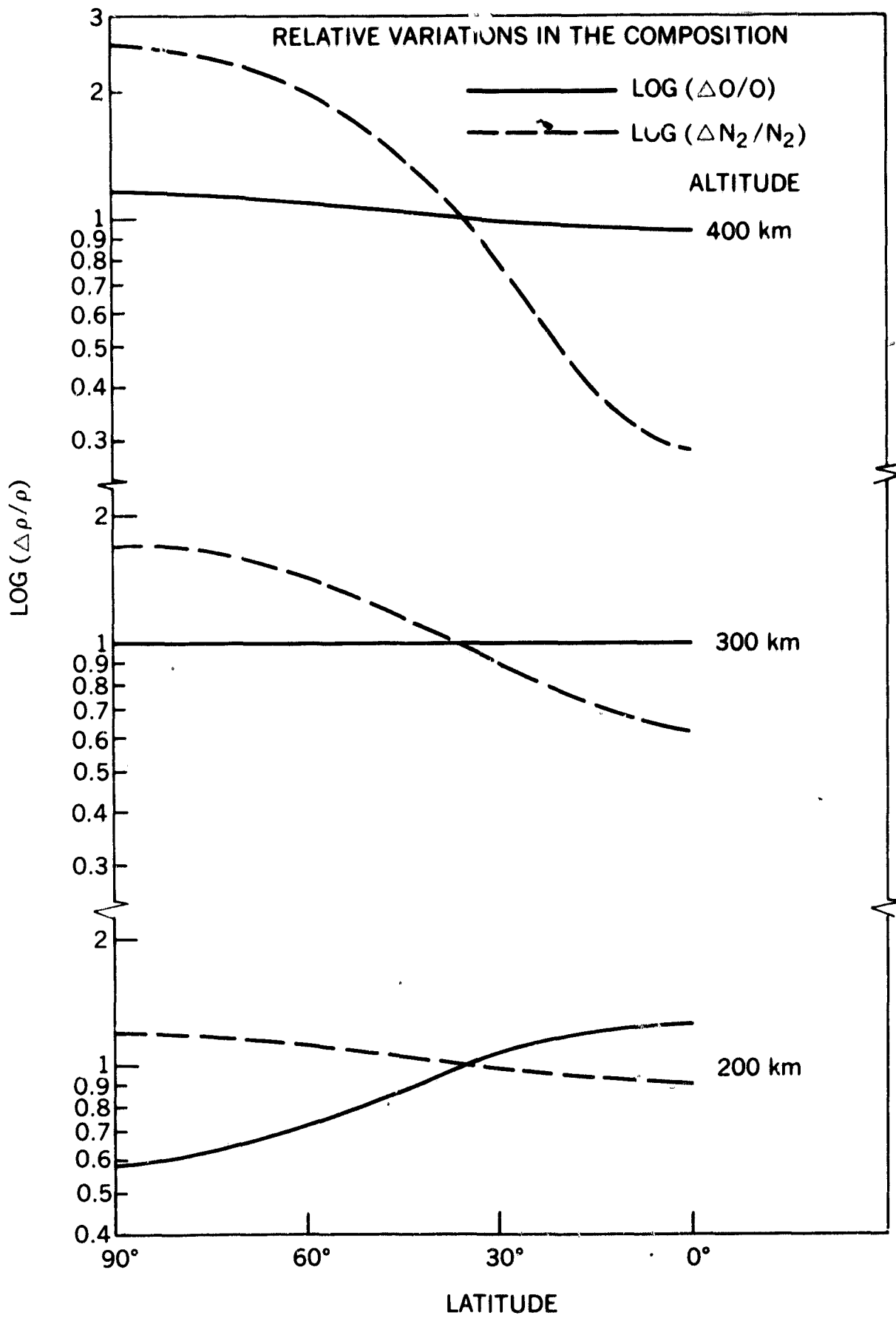


Figure 6. The relative variations of O and N<sub>2</sub> as functions of latitude at different heights. These results agree with observations of the composition and were computed with an energy input that peaks at 150 km suggesting Joule heating as the heating mechanism.

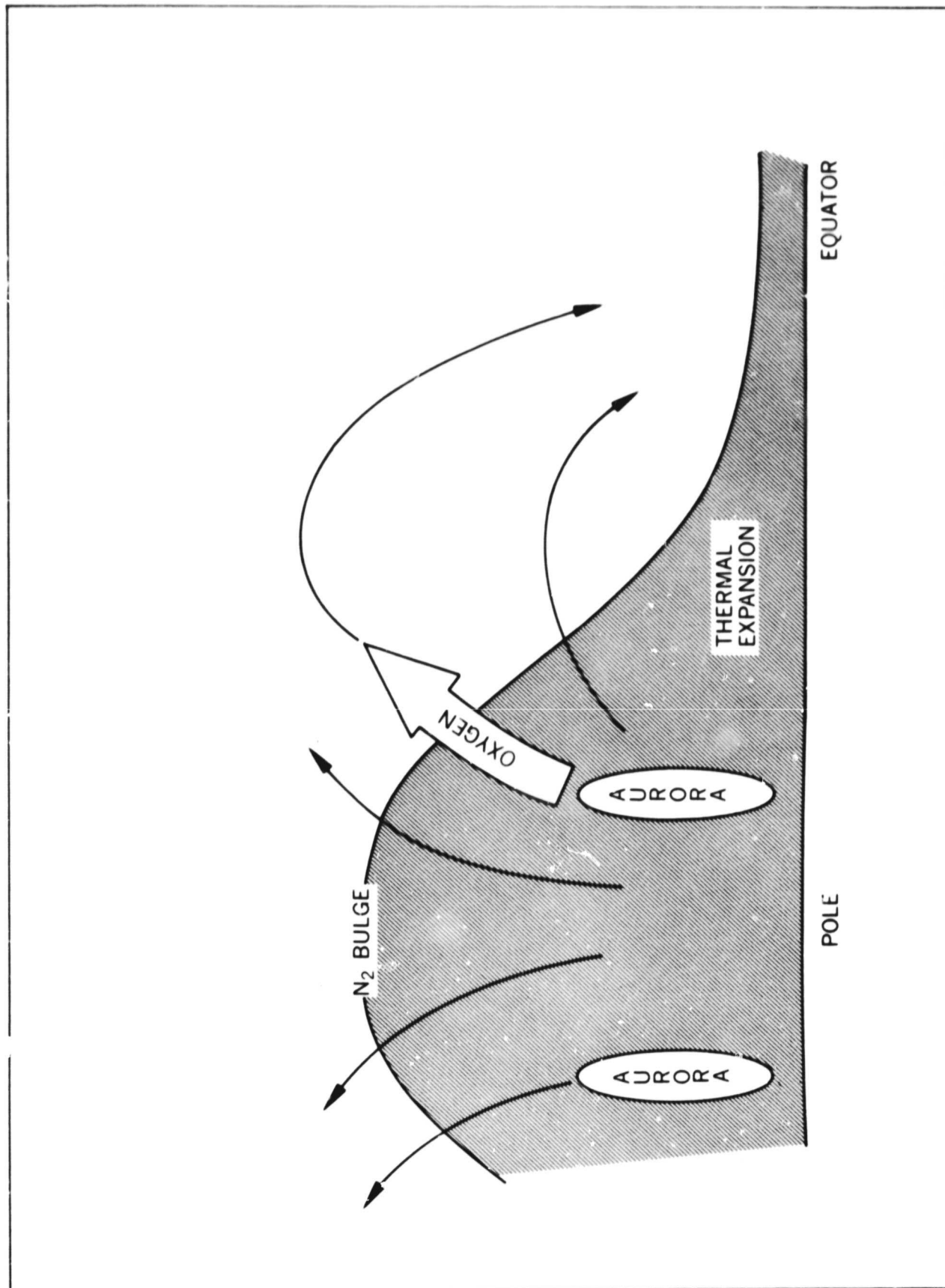


Figure 7. Schematic illustration of the model.